Reversible Data Hiding

Zhicheng Ni, Yun-Qing Shi, Nirwan Ansari, and Wei Su

***Abstract*—A novel reversible data hiding algorithm, which can recover the original image without any distortion from the marked image after the hidden data have been extracted, is presented in this paper. This algorithm utilizes the zero or the minimum points of the histogram of an image and slightly modifies the pixel grayscale values to embed data into the image. It can embed more data than many of the existing reversible data hiding algorithms. It is proved analytically and shown experimentally that the peak signal-to-noise ratio (PSNR) of the marked image generated by this method versus the original image is guaranteed to be above 48 dB. This lower bound of PSNR is much higher than that of all reversible data hiding techniques reported in the literature. The computational complexity of our proposed technique is low and the execution time is short. The algorithm has been successfully applied to a wide range of images, including commonly used images, medical images, texture images, aerial images and all of the 1096 images in CorelDraw database. Experimental results and performance comparison with other reversible data hiding schemes are presented to demonstrate the validity of the proposed algorithm.**

***Index Terms*—Histogram modification, reversible (lossless) data hiding, watermarking.**

I. Introduction

DATA HIDING [1] is referred to as a process to hide data (representing some information) into cover media. That is, the data hiding process links two sets of data, a set of the embedded data and another set of the cover media data. The relationship between these two sets of data characterizes different applications. For instance, in covert communications, the hidden data may often be irrelevant to the cover media. In authentication, however, the embedded data are closely related to the cover media. In these two types of applications, invisibility of hidden data is an important requirement. In most cases of data hiding, the cover media will experience some distortion due to data hiding and cannot be inverted back to the original media. That is, some permanent distortion has occurred to the cover media even after the hidden data have been extracted out. In some applications, such as medical diagnosis and law enforcement, it is critical to reverse the marked media back to the original cover media after the hidden data are retrieved for some legal considerations. In other applications, such as remote sensing and high-energy particle physical experimental investigation, it is also desired that the original cover media can be recovered because of the required high-precision nature. The marking techniques satisfying this requirement are referred to as *reversible*, *lossless*, *distortion-free*, or *invertible* data hiding techniques. Reversible data hiding facilitates immense possibility of applications to link two sets of data in such a way that the cover media can be losslessly recovered after the hidden data have been extracted out, thus providing an additional avenue of handling two different sets of data.

Obviously, most of the existing data hiding techniques are not reversible. For instance, the widely utilized spread-spectrum based data hiding methods (e.g., [2]–[5]) are not invertible owing to truncation (for the purpose to prevent over/underflow) error and round-off error. The well-known least significant bit plane (LSB) based schemes (e.g., [6] and [7]) are not lossless owing to bit replacement without "memory." Another category of data hiding techniques, quantization-index-modulation (QIM) based schemes (e.g., [8] and [9]), are not distortion-free owing to quantization error.

Recently, some reversible marking techniques have been reported in the literature. The first method [10] is carried out in the spatial domain. It uses modulo 256 addition (assuming here that eight-bit grayscale images are considered) to embed the hash value of the original image for authentication. The embedding formula is $Iw = (I + W) \bmod (256)$, in which I denotes the original image, Iw the marked image, and $W = W(H(I), K)$ the watermark, where $H(I)$ denotes the hash function operated on the original image I, and K the secret key. Because of using modulo 256 addition, the over/underflow is prevented and the reversibility is achieved. Some annoying salt-and-pepper noise, however, is generated owing to possible grayscale value flipping over between 0 and 255 in either direction during the modulo 256 addition. The second reversible marking technique was developed in the transform domain [11], which is based on a lossless multiresolution transform and the idea of patchwork [12]. It also uses modulo 256 addition. Note that no experimental results about this technique have been reported. Another spatial domain technique was reported in [13] that losslessly compresses some selected bit plane(s) to leave space for data embedding. Because the necessary bookkeeping data are also embedded in the cover media as an overhead, the method is reversible. Since these techniques [10], [11], [13] aim at authentication, the amount of hidden data is limited. The capacity of method [14], which is based on the idea of patchwork and modulo 256 addition, is also limited except that the hidden data exhibit some robustness against high quality JPEG compression. Since it uses modulo 256 addition, it also suffers from salt-and-pepper noise. As a result, the technique cannot be utilized in many

Manuscript received February 25, 2003; revised June 17, 2005. This work was supported in part by the New Jersey Commission on Science and Technology via NJWINS. This paper was recommended by Associate Editor I. Ahmad.

Z. Ni was with the Department of Electrical and Computer Engineering, New Jersey Institute of Technology, Newark, NJ 07102 USA. He is now with the WorldGate Communications, Inc., Trevose, PA 19053 USA (e-mail: zn2@njit.edu).

Y. Q. Shi and N. Ansari are with the Department of Electrical and Computer Engineering, New Jersey Institute of Technology, Newark, NJ 07102-1982 USA (e-mail: Shi@ADM.njit.edu; nirwan.ansari@njit.edu).

W. Su is with the U.S. Army Communication-Electronics RD&E Center, Intelligence and Information Warfare Directorate, Fort Monmouth, NJ 07703-5211 USA (e-mail: WEI.SU@US.ARMY.MIL).

Digital Object Identifier 10.1109/TCSVT.2006.869964

applications [15]. This observation is valid to all lossless data hiding algorithms that use modulo 256 addition to achieve reversibility.

The first reversible marking technique that is suitable for a large amount of data hiding was presented in [16]. This technique first segments an image into nonoverlapping blocks, and then introduces a discriminating function to classify these blocks into three groups: R(egular), S(ingular), and U(nusable). It further introduces a flipping operation, which can convert an R-block to an S-block and vice versa. A U-block remains intact after the flipping operation. By assigning, say, binary 1 to an R-block and binary 0 to an S-block, all R- and S-blocks are scanned in a chosen sequential order, resulting in a biased (meaning that the binary numbers of 1 and 0 are not balanced) binary sequence. This biased binary sequence is losslessly compressed to leave space for data embedding and the compressed bit sequence is embedded into the cover media as an overhead for later reconstruction of the original image. In data embedding, the R- and S-blocks are scanned once again and the flipping operation is applied whenever necessary to make the changed R- and S-block sequence coincident with the to-be-embedded data followed by the overhead data mentioned above. While it is novel and successful in reversible data hiding, the payload is still not large enough for some applications. Specifically, the embedding capacity estimated by authors ranges from 3 to 41 kb for a $512 \times 512 \times 8$ cover grayscale image when the embedding amplitude is 4 (the estimated average PSNR of the marked image versus the original image is 39 dB) [16]. Another problem with the method is that when the embedding strength increases in order to increase the payload, the visual quality of the marked image will drop severely due to annoying artifacts. To increase the payload dramatically, a new lossless data hiding technique [17] based on integer wavelet transform (IWT) [18], [19] (a second generation wavelet transform, which has avoided round-off errors) was developed recently. Because of the superior decorrelation capability of wavelet transform, the selected bit plane compression of IWT coefficients in high frequency subbands creates more space for data hiding, resulting in a two to five times payload as large as that in [16]. Specifically, its payload ranges from 15 to 94 kb for a $512 \times 512 \times 8$ grayscale image at the same (39 dB) PSNR of the marked images compared with the original images. To achieve reversible data hiding, a histogram modification is applied in its pre-processing to prevent over/underflow. This histogram modification causes, however, a relatively low PSNR of the marked image versus the original image though there are no annoying artifacts. It is noted that reversible data hiding has attracted increasing attention recently, and more algorithms are being developed. A very recent example is the technique reported in [20]. The main idea is that in the embedding phase, the host signal $\mathbf{S}$ is quantized and the residual $\mathbf{r}$ is obtained. Then the authors adopt the CALIC lossless image compression algorithm, with the quantized values as side information, to efficiently compress the quantization residuals to create high capacity for the payload data $\mathbf{h}$. The compressed residual and the payload data are concatenated and embedded into the host signal via generalized-LSB modification method. The payload of this technique is from 15 to 143 kb for a $512 \times 512 \times 8$ grayscale image while the PSNR is 38 dB. Even though the payload is high, the PSNR is still not high enough.

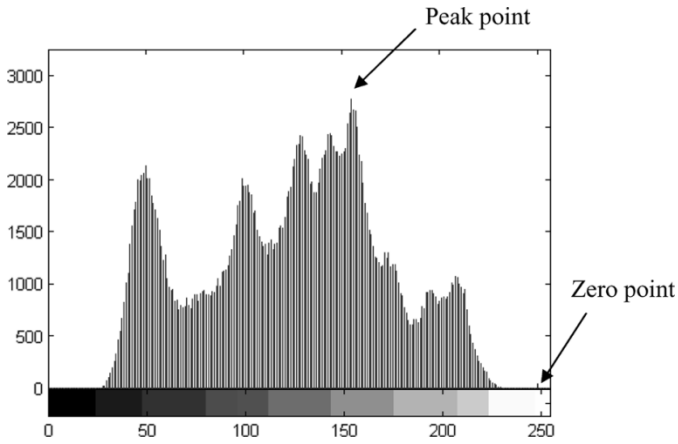

Fig. 1. Histogram of Lena image.

In this paper, we propose a new reversible data embedding technique, which can embed a large amount of data (5–80 kb for a $512 \times 512 \times 8$ grayscale image) while keeping a very high visual quality for all natural images, specifically, the PSNR of the marked image versus the original image is guaranteed to be higher than 48 dB. It utilizes the zero or the minimum point of the histogram (defined below) and slightly modifies the pixel grayscale values to embed data. This technique can be applied to virtually all types of images. Up to now, it has been successfully tested on different types of images, including some commonly used images, medical images, texture images, aerial images, and all of the 1096 images in CorelDRAW database. The computation of our proposed technique is quite simple and the execution time is rather short. Although the proposed lossless data hiding technique is applied to still images, it is also applicable to videos which consist of a sequence of images.

The rest of the paper is organized as follows. The proposed algorithm and its characteristics are described in Section II. Experimental results are presented in Section III, and conclusions are drawn in Sections IV.

II. Algorithm

We first use the "Lena" image as an example to illustrate our algorithm. Then the dada embedding and extracting of the proposed algorithm are presented in terms of pseudocode. Finally, some important issues including data embedding capacity are addressed.

For a given grayscale image, say, the Lena image $(512 \times 512 \times 8)$, we first generate its histogram as shown in Fig. 1.

A. Illustration of Embedding Algorithm Using an Example With One Zero Point and One Peak Point

1) In the histogram, we first find a *zero point*, and then a *peak point*. A zero point corresponds to the grayscale value which no pixel in the given image assumes, e.g., $h(255)$ as shown in Fig. 1. A peak point corresponds to the grayscale value which the maximum number of pixels in the given image assumes, e.g., $h(154)$ as shown in Fig. 1. For the sake of notational simplicity, only one zero point

Fig. 2. Lena image: (a) original, and (b) marked ($\mathrm{PSNR} = 48.2$ dB).

and one peak point are used in this example to illustrate the principle of the algorithm. The objective of finding the peak point is to increase the embedding capacity as large as possible since in this algorithm, as shown below, the number of bits that can be embedded into an image equals to the number of pixels which are associated with the peak point. The implementation of the proposed algorithm with two and more pairs of zero and peak points is further discussed later in this section.

2) The whole image is scanned in a sequential order, say, row-by-row, from top to bottom, or, column-by-column, from left to right. The grayscale value of pixels between 155 (including 155) and 254 (including 254) is incremented by "1." This step is equivalent to shifting the range of the histogram, [155 254], to the right-hand side by 1 unit, leaving the grayscale value 155 empty.
3) The whole image is scanned once again in the same sequential order. Once a pixel with grayscale value of 154 is encountered, we check the to-be-embedded data sequence. If the corresponding to-be-embedded bit in the sequence is binary "1," the pixel value is incremented by 1. Otherwise, the pixel value remains intact. (Note that this step may be included into Step 2, described above. For illustration purposes, we choose to present the embedding algorithm in these three steps.)

The above three steps complete the data embedding process. Now we can observe that the data embedding capacity of this algorithm when only one pair of zero and peak points is used equals to the number of pixels that assume the grayscale value of the peak point as mentioned in Step 1. Fig. 2 shows the original and the marked Lena image, respectively. The histogram of the marked Lena image is displayed in Fig. 3. Note that the peak point, 154, shown in Fig. 1 has disappeared.

B. Pseudocode Embedding Algorithm

Note that zero point defined above may not exist for some image histograms. The concept of minimum point is hence more general. By *minimum point*, we mean such a grayscale value, b, that a minimum number of pixels assume this value, i.e., $h(b)$ is minimum. Accordingly, the peak point discussed above is referred to as *maximum point*. Therefore, in the following discussion, we use terms maximum and minimum points.

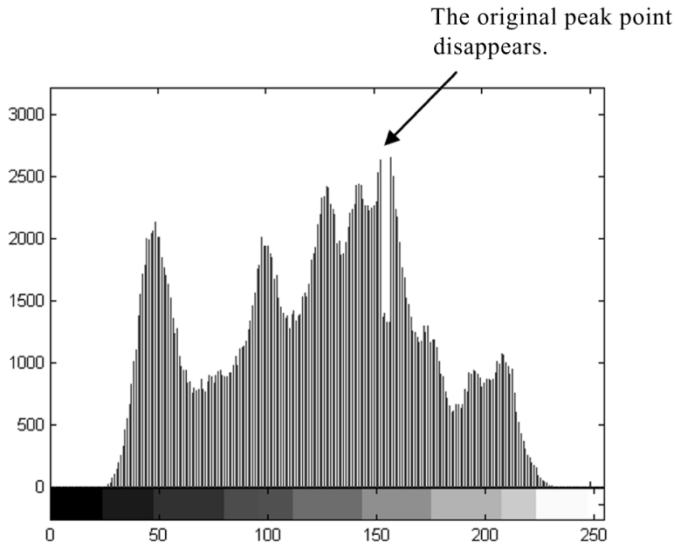

Fig. 3. Histogram of the marked Lena image.

1) Pseudocode Embedding Algorithm With One Pair of Maximum and Minimum Points: For an $M \times N$ image, each pixel grayscale value $x \in [0, 255]$.

1) Generate its histogram $H(x)$.
2) In the histogram $H(x)$, find the *maximum point* $h(a)$ $a \in [0, 255]$ and the *minimum point* zero $h(b)$ $b \in [0, 255]$.
3) If the minimum point $h(b) > 0$, recode the coordinate (i, j) of those pixels and the pixel grayscale value b as overhead bookkeeping information (referred to as overhead information for short). Then set $h(b) = 0$.
4) Without loss of generality, assume $a < b$. Move the whole part of the histogram $H(x)$ with $x \in (a, b)$ to the right by 1 unit. This means that all the pixel grayscale values (satisfying $x \in (a, b)$) are added by 1.
5) Scan the image, once meet the pixel (whose grayscale value is a), check the to-be-embedded bit. If the to-be-embedded bit is "1", the pixel grayscale value is changed to $a + 1$. If the bit is "0", the pixel value remains a.

2) Actual Data Embedding Capacity (Pure Payload): In this way, the *actual data embedding capacity*, C, is calculated as follows:

$$C = h(a) - O \tag{1}$$

where O denotes the amount of data used to represent the overhead information. It is also referred to as pure payload in this paper.

Clearly, if the required payload is greater than the actual capacity, more pairs of maximum point and minimum point need to be used. The embedding algorithm with multiple pairs of maximum point and minimum point is presented below.

3) Pseudocode Embedding Algorithm With Multiple Pairs of Maximum and Minimum Points: Without loss of generality, only a pseudocode embedding algorithm for the case of three pairs of maximum and minimum points is presented below. It is straightforward to generate this code to handle the cases where any other number of multiple pairs of maximum and minimum points is used.

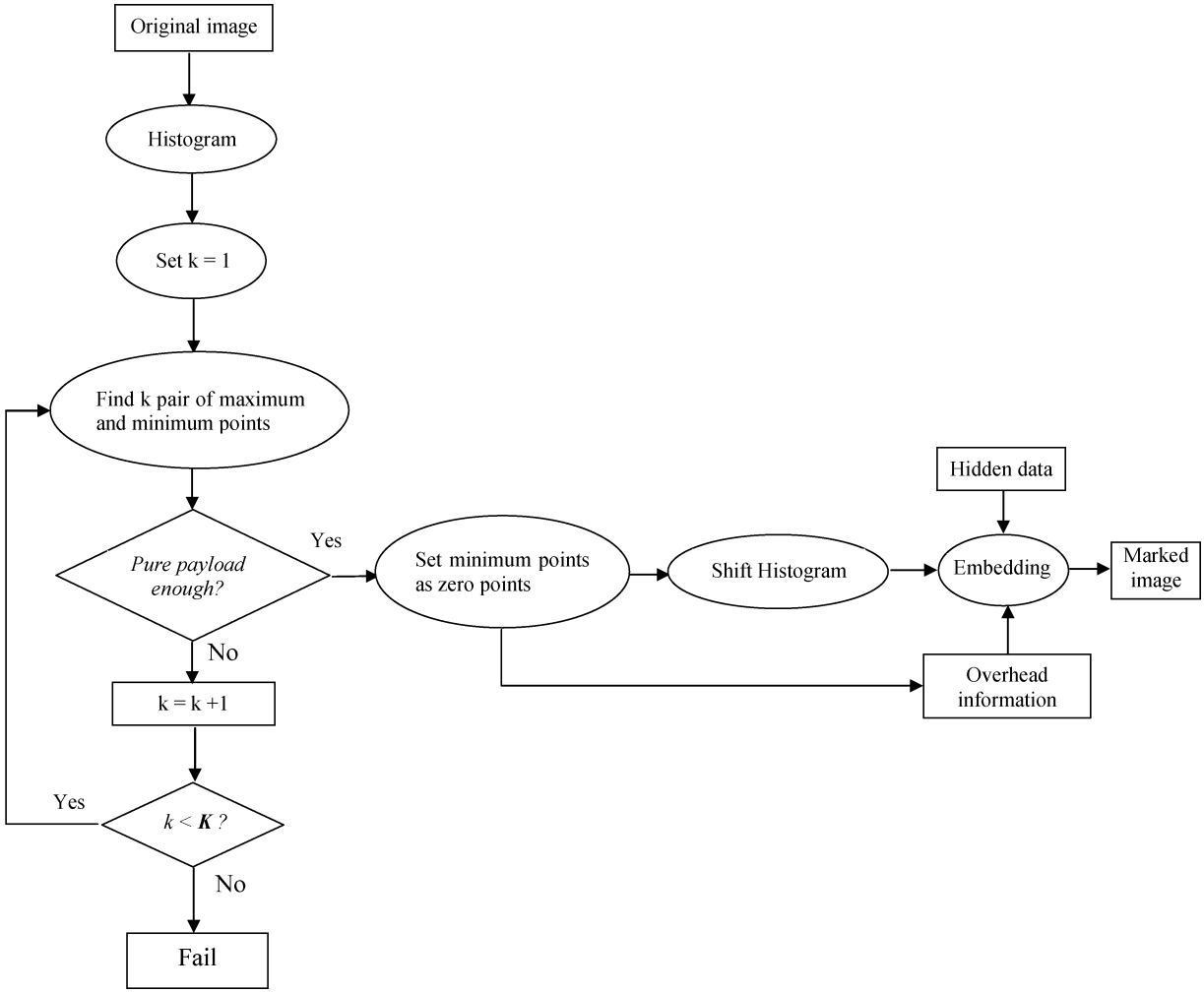

Fig. 4. Data embedding algorithm.

For an $M \times N$ image with pixel grayscale values $x \in [0, 255]$.

1) Generate its histogram $H(x)$.
2) In the histogram $H(x)$, find three minimum point $h(b_1)$, $h(b_2)$, $h(b_3)$. Without loss of generality, assume three minimum points satisfy the following condition: $0 < b_1 < b_2 < b_3 < 255$.
3) In the intervals of $(0, b_1)$ and $(b_3, 255)$, find the maximum point $h(a_1)$, $h(a_3)$, respectively, and assume $a_1 \in (0, b_1)$, $a_3 \in (b_3, 255)$.
4) In the intervals (b_1, b_2) and (b_2, b_3), find the maximum points in each interval. Assume they are $h(a_{12})$, $h(a_{21})$, $b_1 < a_{12} < a_{21} < b_2$ and $h(a_{23})$, $h(a_{32})$, $b_2 < a_{23} < a_{32} < b_3$.
5) Find a point having a larger histogram value in each of the following three maximum point pairs $(h(a_1), h(a_{12}))$, $(h(a_{21}), h(a_{23}))$, and $(h(a_{32}), h(a_3))$, respectively. Without loss of generality, assume $h(a_1)$, $h(a_{23})$, $h(a_3)$ are the three selected maximum points.
6) Then $(h(a_1), h(b_1))$, $(h(a_{23}), h(b_2))$, $(h(a_3), h(b_3))$ are the three pairs of maximum and minimum points. For each of these three pairs, apply Steps 3-5 described in Section II-B1. That is, we treat each of these three pairs as a case of one pair of maximum and minimum points.

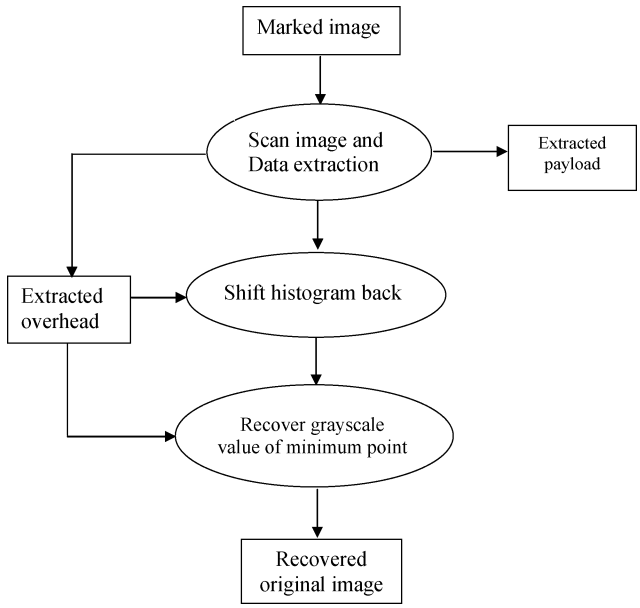

Fig. 5. Data extracting algorithm for one pair of maximum and minimum points.

It is apparent that this embodiment of the proposed algorithm may result in suboptimal performance in terms of the actual

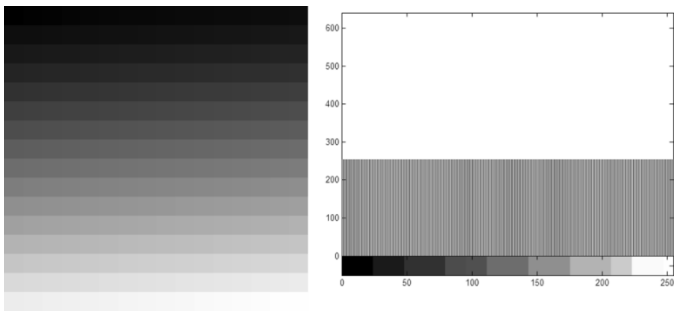

Fig. 6. A man-made image (a) with an exactly horizontal histogram (b).

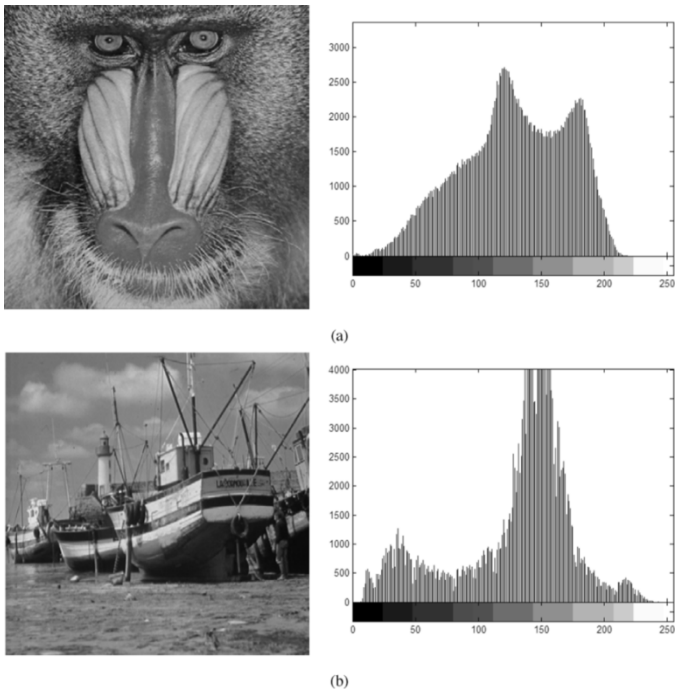

Fig. 7. Some test image examples and their histogram. (a) Baboon; (b) boat; (c) medical image; (d) texture image; (e) CorelDraw image; I; (f) CorelDraw image II; (g) aerial image.

data embedding capacity versus the visual quality of the marked image.

C. Pseudocode Extraction Algorithm

For the sake of brevity, only the simple case of one pair of minimum point and maximum point is described here because, as shown above, the general cases of multiple pairs of maximum and minimum points can be decomposed as a few one pair cases. That is, the multiple pair case can be treated as the multiple repetition of the data extraction for one pair case.

Assume the grayscale value of the maximum point and the minimum points are a and b, respectively. Without loss of generality, assume $a < b$. The marked image is of size $M \times N$, each pixel grayscale value $x \in [0, 255]$.

1) Scan the marked image in the same sequential order as that used in the embedding procedure. If a pixel with its grayscale value $a+1$ is encountered, a bit "1" is extracted. If a pixel with its value a is encountered, a bit "0" is extracted.

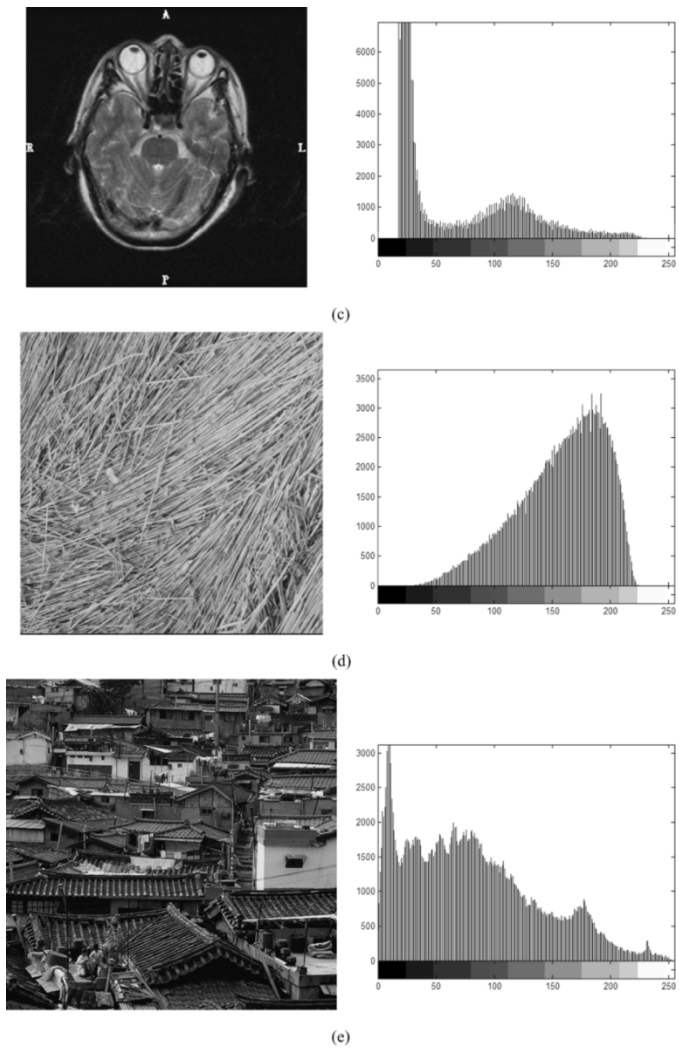

Fig. 7. (cont'd) Some test image examples and their histogram. (a) Baboon; (b) boat; (c) medical image; (d) texture image; (e) CorelDraw image; I; (f) CorelDraw image II; (g) aerial image.

2) Scan the image again, for any pixel whose grayscale value $x \in (a, b]$, the pixel value x is subtracted by 1.
3) If there is overhead bookkeeping information found in the extracted data, set the pixel grayscale value (whose coordinate (i, j) is saved in the overhead) as b.

In this way, the original image can be recovered without any distortion.

D. Embedding and Extraction Flow Charts

In summary, the proposed reversible data hiding and extraction algorithms can be illustrated by the flow charts shown in Figs. 4 and 5, respectively.

E. Lower Bound of the PSNR of a Marked Image Versus the Original Image

The lower bound of the PSNR of a marked image generated by our proposed algorithm versus the original image can be proved larger than 48 dB as follows.

It is clearly observed from the embedding algorithm that the pixels whose grayscale values are between the minimum point and the maximum point will be either added or subtracted by

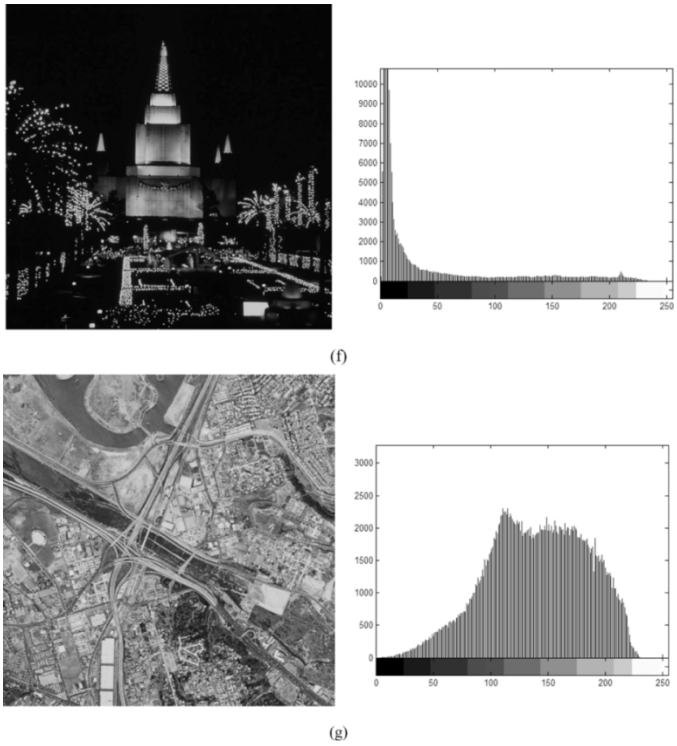

Fig. 7. (cont'd)Some test image examples and their histogram. (a) Baboon; (b) boat; (c) medical image; (d) texture image; (e) CorelDraw image; I; (f) CorelDraw image II; (g) aerial image.

TABLE I
EXPERIMENTAL RESULTS FOR SOME COMMONLY USED IMAGE

Images (512x512)	PSNR of marked image (dB)	Pure payload (bits)
Lena	48.2	5,460
Airplane	48.3	16,171
Tiffany	48.2	8,782
Jet	48.7	59,979
Baboon	48.2	5,421
Boat	48.2	7,301
House	48.3	14,310
Bacteria	48.2	13,579
Blood	48.2	79,460

1 in the data embedding process. Therefore, in the worst case, the grayscale values of all pixels will be either incremented or decremented by 1, implying that the resultant mean square error (MSE) is at most equal to one, i.e., $\mathrm{MSE} = 1$. This leads to the PSNR of the marked image versus the original image being

$$\mathrm{PSNR} = 10 \times \log_{10}\left(\frac{255 \times 255}{\mathrm{MSE}}\right) = 48.13\,\mathrm{dB}. \quad (2)$$

The statement that the lower bound of the PSNR of a marked image generated by our proposed algorithm versus the original image is 48.13 dB has not only been theoretically proved above but also been supported by our numerous experiments. To the best of our knowledge, this resultant lower bound of PSNR is much higher than that of all reversible data hiding techniques reported in the literature.

TABLE II
TEST RESULTS FOR EIGHT MEDICAL IMAGES

Images (512×512)	PSNR of marked image (dB)	Pure payload (bits)
Mpic1	48.2	72554
Mpic2	48.3	184,442
Mpic3	48.2	48,356
Mpic4	48.2	37,692
Mpic5	48.3	88,224
Mpic6	48.2	151,225
Mpic7	48.2	83,505
Mpic8	48.2	139,626

TABLE III
TEST RESULTS FOR SIX TEXTURE IMAGES

Images (512×512)	PSNR of marked image (dB)	Pure payload (bits)
Texture1	48.2	4,017
Texture2	48.3	6,487
Texture3	48.2	6,349
Texture4	48.2	11,131
Texture5	48.3	7,923
Texture6	48.2	10,246

TABLE IV
TEST RESULTS FOR SIX AERIAL IMAGES

Images (1024×1024)	PSNR of marked image (dB)	Pure payload (bits)
Aerial 1	48.2	54,265
Aerial 2	48.2	41,457
Aerial 3	48.2	46,978
Aerial 4	48.2	38,734
Aerial 5	48.3	56,853
Aerial 6	48.2	35,287

TABLE V
TEST RESULTS FOR ALL OF THE 1096 IMAGES IN CORELDRAW DATABASE

Images (512×768)	PSNR of marked image (dB)	Pure payload (bits)		
		Max	Min	Avg.
	48.2	59,262	6,115	18,263

F. Applicability

Where the maximum points and minimum points of a given image histogram are located, the right side, the left side or the middle, is not important for the applicability of this proposed reversible data hiding algorithm. Instead, the key issue is if the histogram has maximum and minimum points, i.e., if the histogram changes up-and-down enough. An extreme example in which the proposed algorithm does not work is an image having an exactly horizontal histogram. One of such a man-made image example is shown in Fig. 6. Loosely speaking, the more dramatically changing in amplitude (i.e., in vertical direction) a given histogram is, the larger the data embedding capacity is.

TABLE VI
OVERALL COMPARISON BETWEEN OTHER REVERSIBLE MARKING METHODS [10], [11], [13], [14], [16], [17] AND OUR PROPOSED METHOD. NOTE THAT THE PURE PAYLOAD AND THE PSNR OF GOLJAN'S METHOD ARE ESTIMATED AVERAGED VALUES WHEN THE EMBEDDING AMPLITUDE IS FOUR

Methods	Pure payload in a 512×512×8 image (bits)	PSNR of marked image (dB)
Honsinger et al.'s [10]	<1024	Not mentioned
Macq and Deweyand [11]	<2,046	Not mentioned
Fridrich et al.'s's [13]	1024	Not mentioned
Goljan et al.'s [16]	3k-41k	39
Vleeschouwer et al.'s [14]	<4096	< 35
Xuan et al.'s [17]	15k-94k	24-36
Celik et al.'s [20]	15-143k	38
Proposed	5k-80k	>48

TABLE VII
COMPARISON BETWEEN OTHER REVERSIBLE MARKING METHODS AND OUR PROPOSED METHOD ON TWO TYPICALLY DIFFERENT IMAGES: LENA AND BABOON. NOTE THAT THE PURE PAYLOAD AND THE PSNR OF GOLJAN *et al.*'S METHOD ARE ESTIMATED AVERAGED VALUES WHEN THE EMBEDDING AMPLITUDE IS FOUR, AND THE DATA OF VLEESCHOUWER *et al.*'S METHOD IS OBTAINED BY USING OUR IMPLEMENTATION OF THEIR ALGORITHM

	Lena (512×512×8)		Baboon (512×512×8)	
Method	Pure payload (bits)	PSNR (dB)	Pure payload (bits)	PSNR (dB)
Honsinger et al.'s	<1024	Not mentioned	<1024	Not mentioned
Macq and Deweyand	<2048	Not mentioned	<2048	Not mentioned
Fridrich et al.'s	1024	Not mentioned	1024	Not mentioned
Goljan et al.'s	24,108	39	2,905	39
Vleeschouwer et al.'s	1024	30	1024	29
Xuan et al's	85,507	36.6	14,916	32.8
Celik et al.'s	74,600	38	15,176	38
Proposed	5,460	48.2	5,421	48.2

G. Computational Complexity

The computational load of the proposed algorithm is light since it does not need to apply any transform such as discrete cosine transform (DCT), discrete wavelet transform (DWT), and fast Fourier transform (FFT). All the processing is in the spatial domain. The required processing mainly lies on generating histogram, determining minimum and maximum (and possibly subminimum and submaximum) points, scanning pixels, and adding or subtracting pixel grayscale values by one in the spatial domain. Hence, the execution time of the algorithm is rather short. Assume the image height is M and the width is N. For one pair of minimum and maximum points, we need to scan the whole image three times in the embedding as discussed in the data embedding. Hence, the computational complexity is $O(3MN)$. Since the multiple pair case is just a multiple repetition of the one pair case, the total computation complexity is $O(3kMN)$ suppose there are k pairs. With a computer Intel Celeron 1.4 GHz and the software Matlab 6.5, the total embedding time needed for the Lena image $(512 \times 512 \times 8)$ is just 100 ms.

III. EXPERIMENTAL RESULTS AND COMPARISON

The proposed reversible data hiding algorithm has been applied to many different types of images, including some commonly used images, medical images, texture images, aerial images, and all of the 1096 images in the CorelDRAW database, and has always achieved satisfactory results, thus demonstrating its general applicability. Here, the results of different kinds of images with different typical histogram distribution are presented (Fig. 7). In all experiments, two pairs of maximum and minimum points are utilized in data embedding and extraction. Note that in Tables I–V, the listed payload is

the pure payload, i.e., the amount of overhead information has been excluded.

Overall comparison between the existing reversible marking techniques and the proposed technique in terms of pure payload and the PSNR is presented in Table VI. Comparison results on two typically different images, Lena and Baboon, which often lead to different data embedding performances, are presented in Table VII. From these comparisons, it is observed that our proposed technique has achieved the highest lower bound of the PSNR with a quite large data embedding capacity.

IV. Conclusions

Our proposed reversible data hiding technique is able to embed about 5–80 kb into a $512 \times 512 \times 8$ grayscale image while guaranteeing the PSNR of the marked image versus the original image to be above 48 dB. In addition, this algorithm can be applied to virtually all types of images. In fact, it has been successfully applied to many frequently used images, medical images, texture images, aerial images, and all of the 1096 images in the CorelDRAW database. Furthermore, this algorithm is quite simple, and the execution time is rather short. Therefore, its overall performance is better than many existing reversible data hiding algorithms. It is expected that this reversible data hiding technique will be deployed for a wide range of applications in the areas such as secure medical image data systems, and image authentication in the medical field and law enforcement, and the other fields where the rendering of the original images is required or desired.

References

[1] W. Zeng, "Digital watermarking and data hiding: technologies and applications," in *Proc. Int. Conf. Inf. Syst., Anal. Synth.*, vol. 3, 1998, pp. 223–229.

[2] J. Cox, J. Kilian, T. Leighton, and T. Shamoon, "Secure spread spectrum watermarking for multimedia," *IEEE Trans. Image Process.*, vol. 6, no. 12, pp. 1673–1687, Dec. 1997.

[3] A. Z. Tirkel, C. F. Osborne, and R. G. Van Schyndel, "Image watermarking-a spread spectrum application," in *Proc. IEEE 4th Int. Symp. Spread Spectrum Techn. Applicat.*, vol. 2, Sep. 1996, pp. 785–789.

[4] J. Huang and Y. Q. Shi, "An adaptive image watermarking scheme based on visual masking," *Electron. Lett.*, vol. 34, no. 8, pp. 748–750, 1998.

[5] J. Huang, Y. Q. Shi, and Y. Shi, "Embedding image watermarks in DC component," *IEEE Trans. Circuits Syst.: Video Technol.*, vol. 10, no. 6, pp. 974–979, Sep. 2000.

[6] J. Irvine and D. Harle, *Data Communications and Networks: An Engineering Approach*. New York: Wiley, 2002.

[7] M. M. Yeung and F. C. Mintzer, "Invisible watermarking for image verification," *Electron. Imag.*, vol. 7, no. 3, pp. 578–591, Jul. 1998.

[8] B. Chen and G. W. Wornell, "Quantization index modulation: a class of provably good methods for digital watermarking and information embedding," *IEEE Trans. Inf. Theory*, vol. 47, no. 4, pp. 1423–1443, May 2001.

[9] F. Perez-Gonzlez and F. Balado, "Quantized projection data hiding," in *Proc. IEEE Int. Conf. Image Process.*, vol. 2, Sep. 2002, pp. 889–892.

[10] C. W. Honsinger, P. Jones, M. Rabbani, and J. C. Stoffel, "Lossless Recovery of an Original Image Containing Embedded Data," U.S. Patent 6 278 791 B1, Aug. 21, 2001.

[11] B. Macq and F. Deweyand, "Trusted headers for medical images," presented at the *DFG VIII-D II Watermarking Workshop*, Erlangen, Germany, Oct. 1999.

[12] W. Bender, D. Gruhl, N. Morimoto, and A. Lu, "Techniques for data hiding," *IBM Syst. J.*, vol. 35, no. 3–4, pp. 313–336, 1996.

[13] J. Fridrich, M. Goljan, and R. Du, "Invertible authentication," in *Proc. SPIE Security Watermarking Multimedia Contents*, San Jose, CA, Jan. 2001, pp. 197–208.

[14] C. De Vleeschouwer, J. F. Delaigle, and B. Macq, "Circular interpretation on histogram for reversible watermarking," in *IEEE Int. Multimedia Signal Process. Workshop*, France, Oct. 2001, pp. 345–350.

[15] Y. Q. Shi, Z. Ni, D. Zou, and C. Liang, "Lossless data hiding: fundamentals, algorithms and applications," in *IEEE Int. Symp. Circuits Syst.*, Vancouver, Canada, May 2004, pp. 33–36.

[16] M. Goljan, J. Fridrich, and R. Du, "Distortion-free data embedding," in *Proc. 4th Inf. Hiding Workshop*, Pittsburgh, PA, Apr. 2001, pp. 27–41.

[17] G. Xuan, J. Zhu, J. Chen, Y. Q. Shi, Z. Ni, and W. Su, "Distortionless data hiding based on integer wavelet transform," *IEE Electron. Lett.*, vol. 38, no. 25, pp. 1646–1648, Dec. 2002.

[18] A. R. Calderbank, I. Daubechies, W. Sweldens, and B. Yeo, "Wavelet transforms that map integers to integers," *Appl. Comput. Harmonic Anal.*, vol. 5, no. 3, pp. 332–369, 1998.

[19] I. Daubechies and W. Sweldens, "Factoring wavelet transforms into lifting steps," *J. Fourier Anal. Appl.*, vol. 4, pp. 247–269, 1998.

[20] M. U. Celik, G. Sharma, A. M. Tekalp, and E. Saber, "Reversible data hiding," in *Proc. IEEE Int. Conf. Image Process.*, vol. 2, Sep. 2002, pp. 157–160.

Zhicheng Ni received the B.E. degree in electrical engineering from Southeast University, Nanjing, China, and received the M.E. degree in electrical engineering from Nanyang Technological University, Singapore, in 1994 and 2000, respectively. He received the Ph.D. degree in electrical engineering from New Jersey Institute of Technology, Newark, NJ, in 2004.

From 1994 to 1998, he was an Electronic Engineer in the Power Research Institute, China. He is currently a Senior Research and Software Engineer in WorldGate, Trevose, PA. His research interests include digital watermarking, image data hiding, computer vision, document image processing, authentication, video compression, DSP. He has three patents and three journal papers.

Yun-Qing Shi (M'90–SM'93–F'05) received the B.S. and M.S. degrees from the Shanghai Jiao Tong University, Shanghai, China, and the M.S. and Ph.D. degrees from the University of Pittsburgh, PA.

He joined the Department of Electrical and Computer Engineering, New Jersey Institute of Technology, Newark, NJ, in 1987, where he is currently a Professor. His research interests include visual signal processing and communications, digital multimedia data hiding and information assurance, applications of digital image processing, computer vision and pattern recognition to industrial automation and biomedical engineering, theory of multidimensional systems and signal processing. Some of his research projects are currently supported by several federal and New Jersey State funding agencies. He is an author/coauthor of more than 170 papers in his research areas, a book on image and video compression, three book chapters on image data hiding, and one book chapter on digital image processing. He holds two U.S. patents and has eight U.S. patents pending.

Dr. Shi is an IEEE Fellow for his contribution to multidimensional signal processing, the chairman of Signal Processing Chapter of IEEE North Jersey Section, the founding Editor-in-Chief of Springer LNCS *Transactions on Data Hiding and Multimedia Security*, an Editorial Board Member of *International Journal of Image and Graphics*, a member of IEEE Circuits and Systems Society (CAS-S) Technical Committee of Visual Signal Processing and Communications, Technical Committee of Multimedia Systems and Applications, and Technical Committee of Life Science, Systems and Applications, a member of IEEE Signal Processing Society (SPS) Technical Committee of Multimedia Signal Processing, an Associate Editor of IEEE Transactions on Circuits and Systems—II: Express Briefs. He was an IEEE CAS-S Distinguished Lecturer, a General Co-Chair of IEEE 2002 International Workshop on Multimedia Signal Processing, a formal reviewer of the *Mathematical Reviews*, an Associate Editor of IEEE Transactions on Signal Processing, and the Guest Editor of several special issues on several journals, one of the contributing authors in the area of Signal and Image Processing to the *Comprehensive Dictionary of Electrical Engineering*.

Nirwan Ansari (S'78–M'83–SM'94) received the B.S.E.E. (*summa cum laude*) from the New Jersey Institute of Technology (NJIT), Newark, in 1982, the M.S.E.E. degree from University of Michigan, Ann Arbor, in 1983, and the Ph.D. degree from Purdue University, West Lafayette, IN, in 1988.

He joined the Department of Electrical and Computer Engineering, NJIT, as an Assistant Professor in 1988, and has been a Full Professor since 1997. He authored *Computational Intelligence for Optimization* (Kluwer, 1997) with E.S.H. Hou and translated into Chinese in 2000, and coedited *Neural Networks in Telecommunications* (Kluwer, 1994) with B. Yuhas. He has frequently been invited to give talks and tutorials. His current research focuses on various aspects of broad-band networks and multimedia communications. He has also contributed over 250 publications in refereed journals, edited books, and conferences.

Dr. Ansari is a Senior Technical Editor of the *IEEE Communications Magazine*, the *ETRI Journal*, and the *Journal of Computing and Information Technology*. He initiated (as the General Chair) the First IEEE International Conference on Information Technology: Research and Education (ITRE2003), was instrumental, while serving as its Chapter Chair, in rejuvenating the North Jersey Chapter of the IEEE Communications Society which received the 1996 Chapter of the Year Award and a 2003 Chapter Achievement Award, served as Chair of the IEEE North Jersey Section and in the IEEE Region 1 Board of Governors during 2001-2002, and has been serving in various IEEE committees including as TPC Chair/Vice-chair of several conferences. He was the 1998 recipient of the NJIT Excellence Teaching Award in Graduate Instruction, and a 1999 IEEE Region 1 Award. He is frequently invited to deliver keynote addresses, tutorials, and talks. He has been selected as an IEEE Communications Society Distinguished Lecturer (2006-2007)..

Wei Su (M'89–SM'95) received the B.S degree in electrical engineering and the M.S degree in systems engineering from Shanghai Jiao Tong University, Shangahi, China, in 1983 and 1997, respectively. He received the M. Eng. degree and the Ph.D. degree in electrical engineering from The City University of New York, New York, in 1992. He also took many graduate courses and conducted research at New Jersey Institute of Technology, Newark, NJ.

He is currently a Research Engineer and Project Leader in the U.S. Army Communication Electronics Research Development and Engineering Center, Fort Monmouth, NJ. His research interests include communication intelligence, signal and image processing, and automatic control.

Dr. Su was a recipient of the 2002 Thomas Alva Edition Patent Award, a recipient of 2004 AOC International Research and Development Award, and a recipient of 2005 Army Research and Development Award.